An attempt to model electrode change during the ESR process

2016 IOP Conf. Ser.: Mater. Sci. Eng. 143 012006

(http://iopscience.iop.org/1757-899X/143/1/012006)

IOP Conf. Series: Materials Science and Engineering **143** (2016) 012006 doi:10.1088/1757-899X/143/1/012006

An attempt to model electrode change during the ESR process

E Karimi-Sibaki [a], A Kharicha[a,b], M Wu[a,b], A Ludwig[b], H Holzgruber[c], B Ofner[c], A Scheriau[c], M Kubin[c], and M Ramprecht[c]

[a]Christian-Doppler Lab for Adv. Process Simulation of Solidification & Melting,
[b]Chair of Simulation and Modeling of Metallurgical Processes,
University of Leoben, Franz-Josef-Str. 18, 8700 Leoben, Austria
[c]INTECO Special Melting Technologies GmbH, 8600 Bruck/Mur, Austria

E-mail: abdellah.kharicha@unileoben.ac.at

Abstract. The electrode change technology is used to produce very large heavy ingots in which a number of electrodes are remelted one after another during the ESR process. Preparing the new electrode for remelting requires a certain period of time when the electric current is stopped (power off). Here, CFD simulation is used to study the behavior of a large scale ESR process during the electrode change (power off). Firstly, the electromagnetic, temperature, and turbulent flow fields in the process before electrode change are modelled. Mold current and thermal effect due to shrinkage of ingot is considered in the model. Then, a transient simulation is performed and the response of the system to the power off is continuously tracked. It is observed that the pool profile of ingot is preserved before and after electrode change. Details of the flow and temperature distributions during electrode change are presented in the paper.

1. Introduction

Nowadays, the demand for very large heavy ingots (> 100 tons) through ESR process is increased especially in chemical, oil and gas industry. Producing a large ingot by ESR process is quite a long process that might take several days. Manufacturing a large ingot requires electrode change technology in which several smaller electrodes are remelted to produce one big ingot. Special care must be taken to avoid internal and surface defects during electrode change due to power interruption in the system.

The entire electrode change procedure is divided to three steps. Firstly, within a very short time (< 5 min), the electric power is turned off, and a new preheated electrode is prepared to replace the remelted last one. Secondly, the electric power is again turned on. Consequently, the temperature of the new electrode rises to reach the melting temperature. Finally, the melt rate increases until reaching the target melt rate. As stated by Holzgruber [1], no traceable change in ingot internal composition was observed during the power interruption. However, Matushkina [2] reported slight defects of surface during electrode change. Jackson [3] monitored thermal field in mold using thermocouples to analyze heat balances across the ingot during power interruption. It was observed that solidification occurred much more rapidly at the pool periphery rather than in the ingot center. It was also found that gross changes in structure and composition of ingot are not expected unless power interruption lasts for too long.

There are only few reports available on this topic. As such, further investigation is required to clarify the influence of power interruption on the process. It is a very first attempt to model electrode change based on CFD simulation. Here, a numerical study is conducted in which the interaction between the turbulent flow, heat, and electromagnetism are taken into account. The model includes the effect of interface motion between molten slag and melt pool. A short collar mold ESR process is studied in which the system behavior is continuously tracked. Formation of surface defects is not explicitly modeled. The thickness of slag skin is kept constant during the whole simulation. This assumption is based on the industrial measurement of skin thickness in plant trial for our case study where a uniformly thin layer is observed along the whole ingot.

Here only results including details of velocity and temperature fields regarding to the first step of electrode change procedure (power off) is presented. The melt pool profile is used as an indicator of the internal quality of ingot. Furthermore, variations in heat fluxes through boundaries are discussed.

2. Model

A 2D axisymmetric computational domain with a short collar mold is considered [4]. The computational domain includes electrode, mold, slag, and ingot. The Finite Volume Method (FVM) is used to model turbulent flow, temperature, and electromagnetic fields. The A-ϕ formulation is applied to compute the electromagnetic field in the whole domain where ϕ is the electric scalar potential and A denotes the magnetic vector potential ($\nabla \times \vec{A} = \vec{B}$). Details of A-ϕ method applied to solve the electromagnetic field for ESR process were described by Kharicha [5]. Note that, the electric current is allowed to cross the slag skin layer entering into the mold before electrode change (power off) [6-9].
After computing the magnetic field (B), the Lorentz force and Joule heating are calculated and added as source terms to momentum and energy equations.

The flow field in slag and melt pool is calculated. The drag resistance of the dendritic mushy zone to the flow is taken into account using the well-known Blake-Kozeny permeability model [10]. Using the previously described model for droplets as mass, momentum, and energy carriers, the impacts of falling droplets are taken into account [11]. Furthermore, the model includes the movement of slag and melt pool interface.
The turbulence is modeled using Scale-Adaptive Simulation (SAS) approach. The advantage of model is the resolution of turbulent spectrum in unstable flow conditions such as interface movement [12].
The temperature field is modeled by solving an enthalpy (h) conservation equation:

$$\frac{\partial}{\partial t}(\rho h) + \nabla \cdot (\rho \vec{u} h) = \nabla \cdot (\lambda \nabla T) + Q + S_{LH} \quad (1)$$

Where (λ) is thermal conductivity, (ρ) is density, (u) is velocity, (T) is temperature, (Q) is Joule heating, and (S_{LH}) is the source term for treating latent heat released by solidification of the ingot:

$$S_{LH} = -\frac{\partial}{\partial t}(\rho f L) - \rho L \vec{u}_{\mathrm{s}} \nabla f \quad (2)$$

In Eq. 2, (L) is latent heat of fusion, (u_{s}) denotes the casting velocity and (f) is the liquid fraction. A constant thickness of slag skin (~ 5 mm) is assumed for the whole simulation. A combined convection-radiation condition is considered for slag free surface where the emissivity coefficient is 0.8. Furthermore, formation of air gap between slag skin layer and mold due to shrinkage of ingot is modeled. For the latter, the contact between slag kin and mold wall is empirically assumed to be lost once the temperature at mold wall becomes 100 K lower than alloy solidus temperature. At the contact region the heat is conducted through slag skin to the mold. Otherwise, a combined radiation-

convection condition is used to model heat transfer through the air gap. Therefore, a fully coupled simulation is performed including the effect of mold current and the thermal effect of solidifying ingot shrinkage. A summary of parameters used in the simulation is described in Table 1.

Table 1. A summary of parameters used in the simulation.

Mater. properties	**Slag**	**Steel**	**Operation parameters**	
Density ($kg.m^{-3}$)	2440	7000	Ingot diam. (m)	1.979
Viscosity (Pa.s)	0.01	0.0062	Elec. diam. (m)	1.1
Specific heat ($J.kg^{-1}$)	1255	500-800	Ingot length (m)	1.245
Liq. therm. cond. ($W.m^{-1}.k^{-1}$)	1.5-5	25-40	Slag height (m)	0.307
Sol. ther. cond. ($W.m^{-1}.k^{-1}$)	0.5	16	Melt rate ($kg.hr^{-1}$)	2200
Ther. exp. Coeff. (K^{-1})	0.0001	0.00011	RMS current (kA)	46
Liquidus temp. (K)	1715	1773	Freq. (Hz)	0.2
Solidus temp. (K)	1598	1668	Power (MW)	2.407
Liq. e. cond. ($ohm^{-1}.m^{-1}$)	180	$8.8x10^5$	Elec. change time (s)	175
Sol. e. cond. ($ohm^{-1}.m^{-1}$)	15	$8.8x10^5$		

First, the process is simulated before electrode change, and temperature, velocity, and electromagnetic fields are obtained. Afterwards, the following conditions are imposed on the system during the first step of electrode change (power off). The electric current is stopped flowing through the system, thus the Lorentz force and Joule heating are vanished. The electrode melting is ceased (no droplets), and subsequently the casting velocity is changed to zero. Additionally, the whole slag surface is considered to be exposed to the air.

3. Results and discussions

Figure 1 shows the modeling results of process before electrode change (power interruption) including magnetic flux density, current density, velocity, temperature, turbulence kinetic energy, and turbulence effective thermal conductivity. The generated power in the process is slightly oscillating around the average value (~ 2.4 MW) due to interface movement. As shown in Figure 1(a), a portion of electric current (~ 5%) enters to the mold in slag zone then returns to ingot through the contact region (mold and melt pool). The standing height (liquid metal in direct contact to mold) is influenced by the mold current [11, 13]. The flow and temperature distributions are shown in Figure 1(b). The flow is rotating clock-wisely (converging flow) under the edge of electrode in the slag zone that indicates the Lorentz force is dominant. However, the flow is governed by thermal buoyancy and droplets impact in the bulk of liquid melt pool. Stronger flow under the shadow of electrode is due to the effect of droplets that bring momentum and thermal energy to melt pool. Furthermore, the movement of slag-melt pool interface certainly intensifies the flow in the liquid melt pool [14]. The maximum elevation of interface is observed to be around 7 mm in the simulation. Kharicha [15] reported a maximum elevation of 30 mm for a smaller scale ESR system (Diam. ~ 0.6 m). Nevertheless, with the increase of system size, the current density which is proportional to the inverse of square of diameter decreases in the domain. As such, a smoother movement of interface is expected. Additionally, the temperature distribution and isolines of solid fraction (indicating pool profile) are shown in Figure 1(b). The temperature field is relatively uniform in the melt pool and slag indicating rigorous mixing in the system. The slag is very hot under the shadow of electrode where the current density and subsequently released Joule heating is high. The distributions of turbulence kinetic energy and turbulence effective thermal conductivity are shown in Figure 1 (c). The turbulence kinetic energy is as notably strong in melt pool as in the slag region. Strong turbulence in liquid melt pool has been also reported by Kharicha [16-17] after simulation of the electrode melting in a fully coupled 3D simulation. It must be noted that a region of intense turbulence is created at upper part of melt pool because of interface

movement. As shown in Figure 1 (c), the effective thermal conductivity of slag can dramatically increase (~ 150 $W.m^{-1}.K^{-1}$) in the bulk due to strong turbulence. Therefore, the energy transfer is efficiently increased, and it leads to relatively uniform temperature in the slag. However, the turbulence is damped near the walls and slag-melt pool interface where the effective thermal conductivity of slag is in the same magnitude of the molecular thermal conductivity (~ 5 $W.m^{-1}.K^{-1}$). Snapshots of flow, temperature, and solidification during the first step of electrode change (power off) are illustrated in Figure. 2. The pool profile is slightly influenced near the mold wall where the cooling rate is large. However, the flow distribution is totally altered. The clock-wise rotating vortex under the edge of electrode (converging flow) disappears in slag zone. During power interruption, the flow is completely driven by buoyance force results in counter-clock wise rotation of flow (diverging flow) in the slag. Furthermore, the magnitude of velocity decreases in the bulk as the time proceeds whereas the flow is still strong near the mold wall due to thermal buoyancy. The temperature response is observed to be much slower than flow response to the power interruption. Based on the simulation result, a minor impact on the pool profile is observed during power interruption.

The heat loss through the slag free surface and mold normalized by their magnitudes before power interruption is plotted against time as shown in Figure. 3. The amount of heat loss through the mold (~ 0.9 MW) remains almost constant since the thickness of slag skin is invariable. However, the heat loss through slag free surface (slag-air interface) during electrode change is notably larger compared to the value before power interruption (~ 0.8 MW). The heat loss through slag free surface is intensified at the beginning of power interruption due to increase in contact area between slag and air. As time proceeds, the temperature of slag at free surface decreases. Consequently, the convective-radiative heat loss at slag free surface is decreasing. Afterwards, increase in heat loss through slag-air interface is observed once again. Because of thermal buoyancy, the colder liquid slag on the slag-air interface sinks whereas hot liquid slag moves toward the free surface. This behavior of flow is clearly demonstrated in Figure 2(e-f).

According to our investigation, it is even possible to solidify slag at the free surface. Nevertheless, it is highly unlikely that solidified slag layers float on the surface because of having higher density compared to the liquid slag. Most probably, the floating solidified slag pieces sink into the hot slag bath where they remelt once again.

Note that the entire electrode change procedure is not only the first step (power off). The procedure also includes heating of the new electrode until reaching melting temperature (second step) and remelting of the electrode until reaching the target melt rate (third step). Generally, those steps take much longer time (~ 30 min) compared to the first step (power off). During second and third steps, operation conditions of process such as input power or melt rate are dynamically changing. Further investigations are required to explore the behavior of the process during second and third steps.

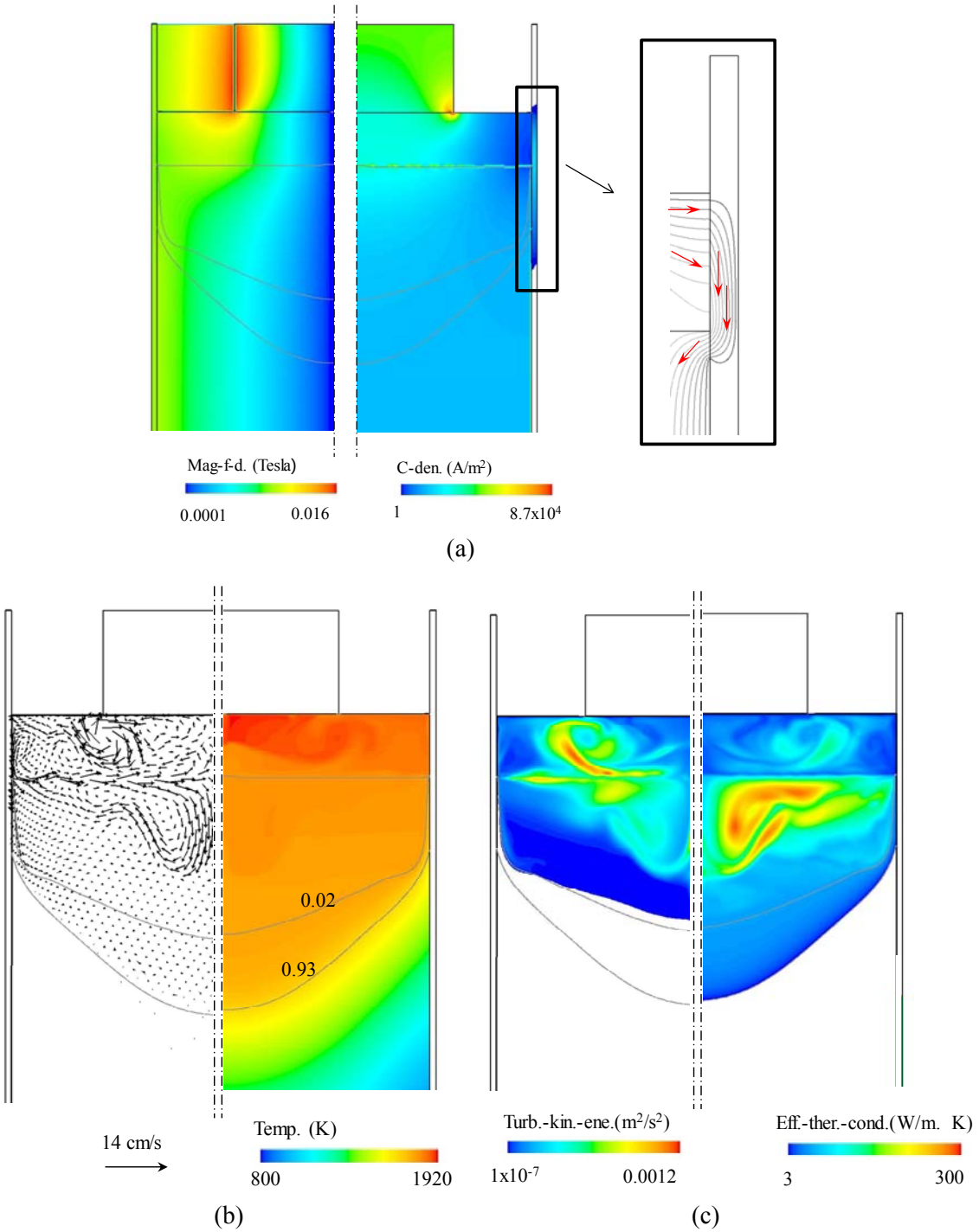

Figure 1. (a) Left: contour of magnetic flux density, Right: contour of electric current density (red arrows show direction of electric current), (b) Left: vectors of velocity, Right: contour of temperature overlaid with isolines of solid fraction, (c) Left: contour of turbulence kinetic energy, Right: contour of turbulence effective thermal conductivity in slag and melt pool.

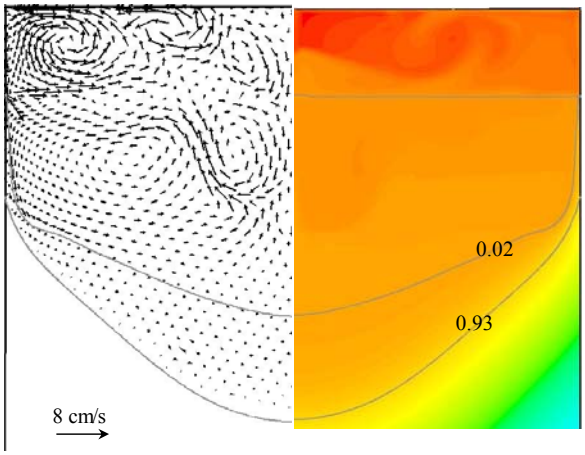

(a) t= 10 s

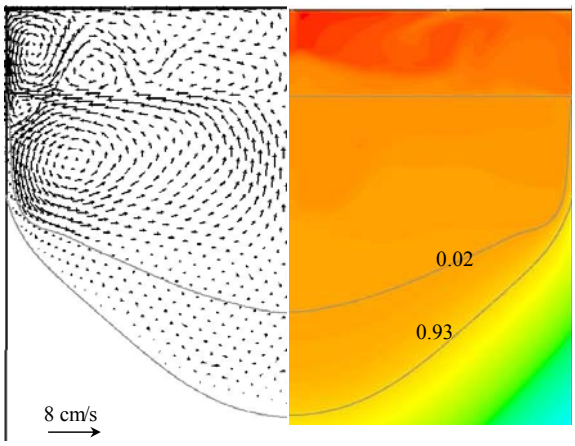

(b) t= 40 s

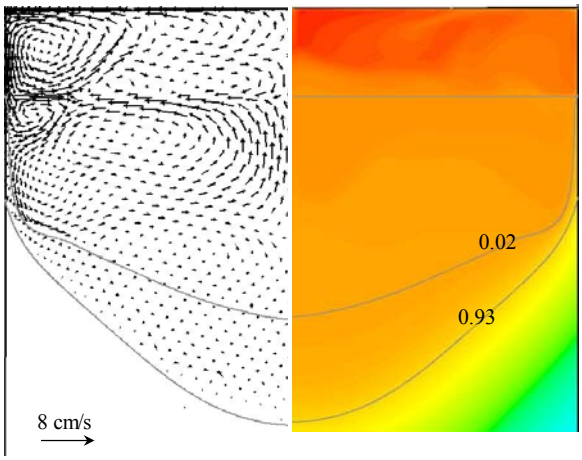

(c) t= 80 s

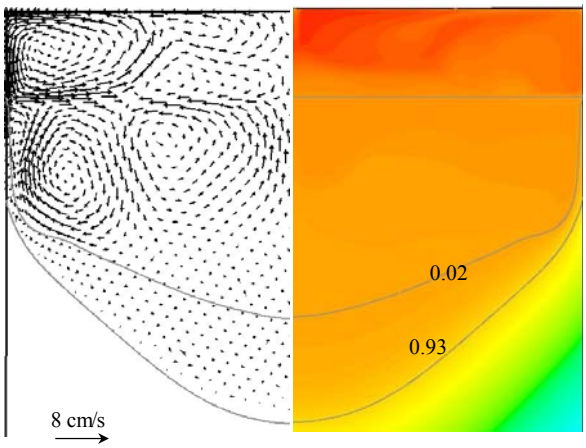

(d) t= 120 s

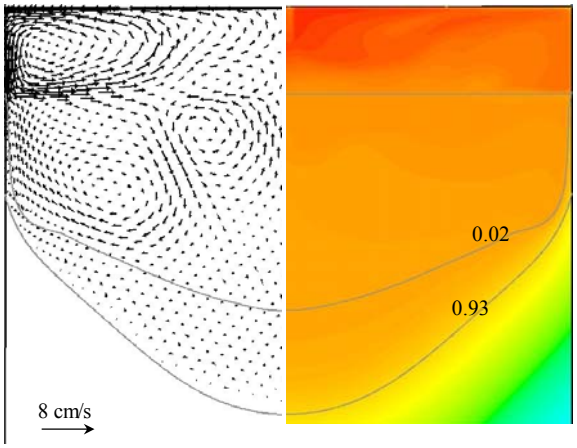

(e) t= 150 s

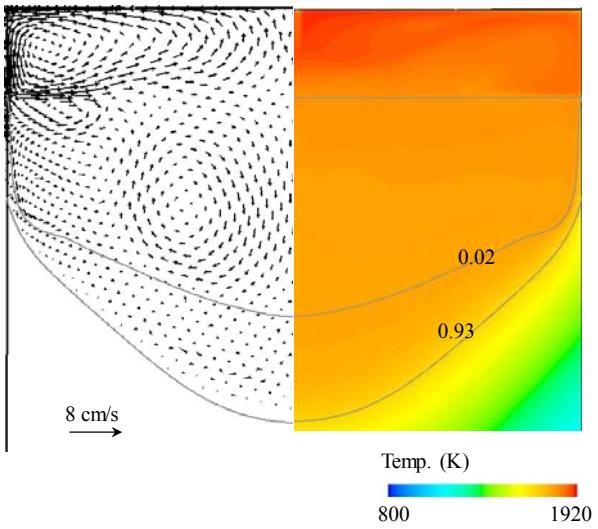

(f) t= 175 s

Figure 2. Snapshots of dynamic change of thermal and velocity fields at different times during power off: (a) t= 10 s, (b) t= 40 s, (c) t= 80 s, (d) t= 120 s, (e) t= 150 s, (f) t= 175 s, Left: vectors of velocity, Right: contour of temperature overlaid with isolines of solid fraction.

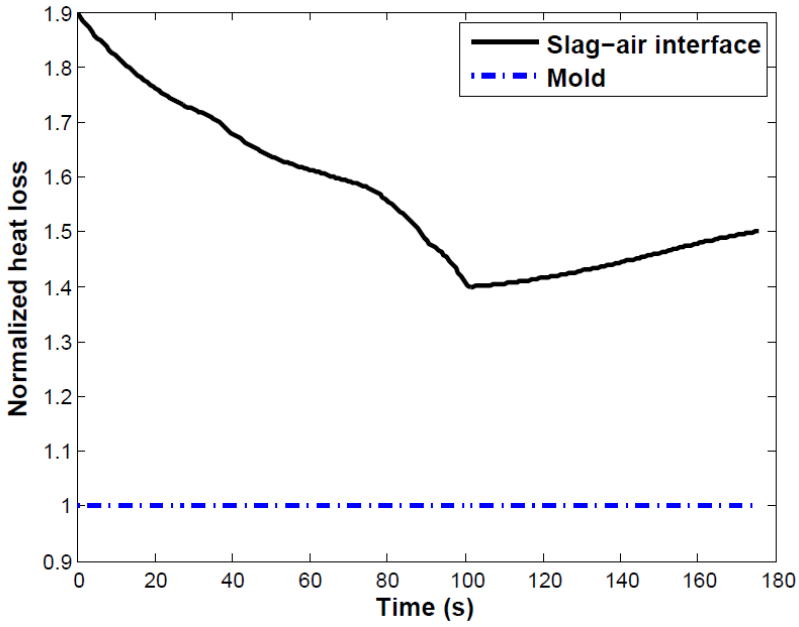

Figure 3. Normalized heat loss through slag-air interface and mold wall is plotted versus time during the first step of electrode change (power off).

4. Summary

Producing a large ingot by ESR process requires electrode change technology in which a number of smaller electrodes are remelted one after another. The electrode change procedure is divided into three steps. Firstly, the electric power is turned off (power off), and the end of remelted electrode is replaced by a new preheated electrode. Secondly, the electric power is turned on again, and the new electrode is heated to its melting temperature. Finally, the new electrode is continuously remelted until reaching target melt rate. Here, the influence of power interruption on a large scale ESR process during the first step of electrode change (power off) is studied using CFD simulation tool. A 2D axisymmetric computational domain is considered where the slag-melt pool interface is allowed to move. The interactions between turbulent flow, electromagnetic, and temperature fields are considered. The current is allowed to flow through the short collar mold used in the process. Additionally, the thermal effect of shrinkage of ingot is taken into account in the model. The behavior of system during electrode change including details of flow, and temperature distributions as well as heat loss through boundaries are discussed. Generally, the pool profile is used as an indication of ingot internal quality. Therefore, preserving the original pool profile before and after power interruption is a symptom of maintaining ingot quality. According to simulation results, changes in pool profile of ingot are insignificant during the short period of electrode change (power off). The current study included only the first step of electrode change procedure. Further investigations are required to explore the behavior of process during second and third step of electrode change procedure.

5. Acknowledgement

The authors acknowledge the financial support by INTECO GmbH and the Austrian Federal Ministry of Economy, Family and Youth and the National Foundation for Research, Technology and Development within the framework of the Christian Doppler Laboratory for Advanced Process Simulation of Solidification and Melting.

6. References

[1] Holzgruber W, Kubisch C, and Jaeger H H 1971 *Neue Hutte* **16** 606
[2] Matushkina L I, Klyuver M, Dedushev L A, Kosyrev L L, Volkov S E, and Sharapov A, 1970 *Sb. Tr. Tsent. Nauch. Issted. Inst Chern. Met.* **75** 167
[3] Jackson R O, Mitchell A, and Luchok J 1972 *J. Vac. Sci. Tech.* **9** 1301
[4] Karimi-Sibaki E, Kharicha A, Korp J, Wu M, Ludwig A 2014 *Mater. Sci. Forum* **790** 396
[5] Kharicha A, Wu M, and Ludwig A 2014 *ISIJ Int.* **54** 1621
[6] Kharicha A, Karimi-Sibaki E, Wu M, and Ludwig A 2013 *Proc. Of LMPC* (New York: Wiley–Interscience) p 95
[7] Karimi-Sibaki E, Kharicha A, Wu M, Ludwig A, Holzgruber H, Ofner B, Ramprecht M 2014 *Proc. of ICRF* (Milan) on data storage device
[8] Kawakami M, Nagata K, Yamamura M, Sakata N, Miyashita Y, and Goto K S 1977 *Testsu-to-Hagane* **63** 220
[9] Holzgruber H, Holzgruber W, Scheriau A, Knabl M, Kubin M, Korp J, Pierer R 2011 *Proc. of LMPC* (Nancy) p 57
[10] Voller V R, and Prakash C 1978 *Int. J. Heat Mass Trans.* **30** 1709
[11] Karimi-Sibaki E, Kharicha A, Wu M, Ludwig A, Holzgruber H, Ofner B, Ramprecht M 2013 *Proc. of LMPC* (New York: Wiley–Interscience) p 13
[12] Menter F R and Egorov Y 2005 *AIAA paper 2005-1095, Reno/NV*
[13] Kharicha A, Schutzenhofer W, Ludwig A, Tanzer R, Wu M 2007 *Proc. of STEEL SIM* (Graz) p 105
[14] Kharicha A, Ludwig A, Wu M 2005 *Mater. Sci. Eng. A* **413-414** 129
[15] Kharicha A, Ludwig A, Wu M 2011 *Proc. of LMPC* (Nancy) p 41
[16] Kharich A, Ludwig A, and Wu M 2011 *EPD congress* (San Diego) p 771
[17] Kharicha A, Wu M, Ludwig A, Ramprecht M, Holzgruber H 2012 *CFD modelling and simulation in materials* (New York: Wiley–Interscience) p 139